Journal Name

ARTICLE TYPE

Cite this: DOI: 00.0000/xxxxxxxxxx

Influence of local microenvironment on the double hydrogen transfer in porphycene†

Piotr Kasprzycki,[a,b] Przemysław Kopycki,[a,‡] Arkadiusz Listkowski,[b,c] Aleksander Gorski,[b] Czesław Radzewicz,[a] David J. S. Birch,[d] Jacek Waluk,[*,b,c] Piotr Fita,[*,a]

Received Date
Accepted Date

DOI: 00.0000/xxxxxxxxxx

We carried out time-resolved transient absorption and fluorescence anisotropy measurements in order to study tautomerization of porphycene in rigid polymer matrices at cryogenic temperatures. Studies were carried out in poly(methyl methacrylate) (PMMA), poly(vinyl butyral) (PVB), and poly(vinyl alcohol) (PVA).The results prove that in all studied media hydrogen tunnelling plays a significant role in the double hydrogen transfer which becomes very sensitive to properties of the environment below approx. 150 K. We also demonstrate that there exist two populations of porphycene molecules in rigid media: „hydrogen-transferring" molecules, in which tautomerization occurs on time scales below 1 ns and „frozen" molecules in which double hydrogen transfer is too slow to be monitored with nanosecond techniques. The number of „frozen" molecules increases when the sample is cooled. We explain this effect by interactions of guest molecules with a rigid host matrix which disturbs symmetry of porphycene and hinders tunnelling. Temperature dependence of the number of hydrogen-transferring molecules suggests that the factor which restores the symmetry of the double-minimum potential well in porphycene are intermolecular vibrations localized in separated regions of the amorphous polymer.

Introduction

Proton and hydrogen transfer reactions are deceptively simple processes because they involve the most basic chemical element. Nevertheless, quantitative description of such reactions remains challenging due to factors such as quantum phenomena, involvement of the transferred atom in hydrogen bonds or coupling of reaction coordinates to molecular vibrations [1–4]. At the same time reactions involving hydrogen transfer are extremely widespread both in nature and in artificial chemical systems. In the first place they underlie the molecular machinery of life, occurring during numerous enzyme-catalysed reactions [5–7] or DNA mutation processes [8–10]. On the other hand, hydrogen rearrangement is considered as a promising mechanism underlying operation of molecular switches – basic components used in the emerging field of nanoelectronics [11].

The phenomenon of quantum tunnelling which frequently manifests itself during proton or hydrogen transfer due to relatively low mass of the transferred particle, may drastically alter the outcome of a reaction compared to its classical description and allow reactions that would not occur without it. Tunnelling plays a key role even in relatively simple processes such as light-induced intramolecular reorganization of benzene derivatives [12] or – very important in organic synthesis – elimination reaction moderated by the hydroxyl ion [13] as well as in many other organic reactions [14]. It has been pointed out that better understanding of tunnelling in proton or hydrogen transfer reactions may create a chance for innovations such as an efficient control of the reactions' course [15], artificial (more efficient) enzymes [16] or fast charging lithium–ion batteries [17]. Therefore, a constant effort is put into development of more accurate models that can be used to describe proton and hydrogen transfer reactions [7,18–33]. Consequently, the experimental data that can be used to verify new models can be invaluable. This work belongs to this trend.

Porphycene (Pc) – the first synthetic structural isomer of well-known porphyrin – proved to be a very convenient system for studying the hydrogen transfer. In an isolated porphycene molecule the *trans* form, with the internal hydrogen atoms occupying positions along one of the two diagonals of the molecule, is the most stable tautomer. Two equivalent *trans* forms of the molecule make it a symmetric double-minimum potential well for the motion of hydrogen atoms. The substrate and the product of the transfer reaction are chemically identical in this case (Fig. 1).

The double hydrogen transfer in porphycene and its derivatives has been extensively studied both theoretically [24,25,27,30,34–37] and experimentally. In the latter case the range of phases in which the dynamics of tautomerization was studied includes crystals [38–41], solutions [42–46] and single

[a] *Institute of Experimental Physics, Faculty of Physics, University of Warsaw, Pasteura 5, 02-093 Warsaw, Poland*
[b] *Institute of Physical Chemistry, Polish Academy of Sciences, 44/52 Kasprzaka, Warsaw 01-224, Poland*
[c] *Faculty of Mathematics and Science, Cardinal Stefan Wyszyński University, Dewajtis 5, 01-815 Warsaw, Poland*
[d] *Photophysics Group, Centre for Molecular Nanometrology, Department of Physics, Scottish Universities Physics Alliance,University of Strathclyde, 107 Rottenrow East, Glasgow G4 0NG, U.K.*

† Electronic Supplementary Information (ESI) available: Sample preparation details, experimental procedures, additional data. See DOI: 00.0000/00000000.

‡ Present address: Department of Optics, University of Valencia, C/ Dr. Moliner, 50, E-46100 Burjassot, Spain.
* E-mails: Jacek Waluk – jwaluk@ichf.edu.pl, Piotr Fita – fita@fuw.edu.pl

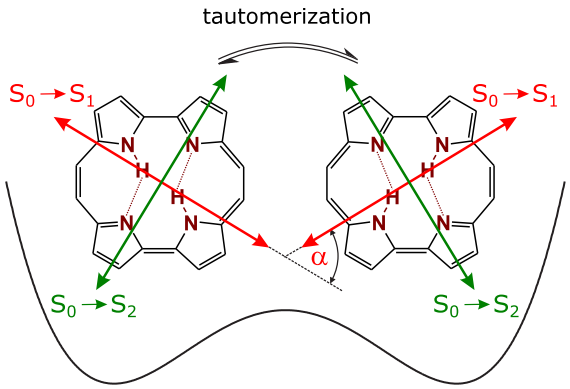

Fig. 1 Scheme of the double hydrogen transfer in porphycene. Approximate orientations of $S_0 \rightarrow S_1$ and $S_0 \rightarrow S_2$ dipole transition moments are also shown.

molecules[47–53]. Recently, the potential for molecular switching induced by various stimuli at low temperatures has been also demonstrated for porphycene and it has been predicted that it should be possible to achieve this effect even at room temperature[11].

The method for studying tautomerization of porphycene and its derivatives in condensed phases is based on the fact that the double hydrogen transfer is accompanied by rotation of dipole transition moments. This fact makes polarization-sensitive optical spectroscopy techniques, such as fluorescence anisotropy measurements or pump-probe experiments with linearly polarized pulses, useful methods for reaction rate measurements[45,54]. When a Pc sample is excited with a short pulse of linearly polarized light a population of molecules with the transition moments oriented preferentially along the electric field vector of the excitation light is selected. The double hydrogen transfer leads to reorientation of the transition moments, which can be detected either by monitoring the polarization of fluorescence emitted by the sample or by probing the excited sample with another linearly polarized light pulse. In either case appropriate time-dependent signals (fluorescence intensity or optically induced absorbance change) are recorded for two polarizations, parallel and perpendicular with respect to the polarization of the excitation light, $S_{\parallel}(t)$ and $S_{\perp}(t)$, respectively. From these two quantities anisotropy of the signal $r(t)$ is calculated using the formula

$$r(t) = \frac{S_{\parallel}(t) - S_{\perp}(t)}{S_{\parallel}(t) + 2S_{\perp}(t)} \tag{1}$$

When the studied process is *trans-trans* tautomerization of a molecule in which the symmetry ensures equivalency of the two *trans* positions, the temporal dependence of anisotropy is described by an exponential decay[45],

$$r(t) = (r_0 - r_\infty)\exp(-2kt) + r_\infty \tag{2}$$

where k is the tautomerization rate, and r_0 and r_∞ are initial and asymptotic anisotropy values, respectively. Exact values of r_0 and r_∞ depend on the angle α (Fig. 1) by which the transition moments rotate, and on the selection of electronic states that are excited and probed in the experiment. For experiments carried out in solutions rotational diffusion also leads to the decay of anisotropy. If the time scale of rotational diffusion is comparable to hydrogen transfer times, equation (2) must be modified in order to take this effect into account. It has been experimentally verified that in the case of porphycene solutions a simple multiplication of equation (2) by an exponential decay is sufficient:

$$r(t) = [(r_0 - r_\infty)\exp(-2kt) + r_\infty]\exp(-t/\theta) \tag{3}$$

where θ denotes the rotational diffusion time.

If more than one population of molecules contributes to the signal, the measured anisotropy can be described as a weighted sum of anisotropy values for each contributing population[55]:

$$r(t) = \sum_i f_i r_i(t) \tag{4}$$

where $r_i(t)$ describe temporal dependence of anisotropy for each population and f_i are normalized weights that satisfy the condition $\sum_i f_i = 1$.

The above fact allowed determination of tautomerization rates in both the electronic ground state S_0 and the first singlet excited state S_1 of numerous porphycenes by recording anisotropy decays in pump-probe (transient absorption) experiments, where the excitation pulse transferred molecules from S_0 to S_1 and both states were probed simultaneously by a probe pulse with an appropriate wavelength[42–46].

Before time-resolved studies of the double hydrogen transfer in porphycenes were undertaken, a similar concept was applied to derive information on tautomerization rates from steady-state fluorescence anisotropy measurements[54]. In this case time-averaged values of anisotropy weighted with fluorescence intensity were measured and the technique allowed determination of temperature dependence of the double hydrogen transfer rate under cryogenic conditions. It turned out to correspond to a thermally-activated process with activation energy much lower than the predicted height of the barrier that separates the potential minima of the double well. On the other hand, it was equal to the energy of one of the low-frequency vibrations of porphycene (a_g symmetry, 180 cm^{-1}), which strongly modulates the distance between nitrogen atoms that are the donor and the acceptor of the transferred hydrogen atom. Moreover, vibrational mode-dependent tunnelling splittings have been observed for Pc isolated in supersonic jets[56,57] and helium nanodroplets[58], with the largest splitting observed for the excited state of the 180 cm^{-1} vibration. Altogether, the above mentioned results led to a hypothesis that tautomerization of porphycene involves tunnelling of hydrogen atoms through the potential barrier and is promoted by excitation of the vibration that modulates this barrier.

In subsequent works this conclusion was strongly supported by transient absorption anisotropy measurements carried out in a broad temperature range. Analysis of the temperature dependence of tautomerization rates showed that the thermal activation of the first vibrationally excited state of the 180 cm^{-1} a_g vibration significantly speeds up the double hydrogen transfer[46]. Recently, a more complicated picture of the coupling between vibrations and tautomerization emerged from measurements of Raman spectra of dimers of terephthalic acid[1,3]. It has been shown that freezing out of the vibration that modulates the barrier width leads to an increase of the barrier transmission and results in an increase of the intrinsic tunnelling rate. Observation of this effect was possible because vibrational frequencies directly measured in these works were sensitive to delocalization of the hydrogen wavefunction between the two potential minima. Such an effect should be expected also in the case of porphycene[24], but anisotropy measurements applied in porphycene studies are sensitive only to hydrogen jumps (localization of the wavefunction in one of the minima). Thus, the situation is simplified and the effects seen by the Raman spectroscopy of terephthalic acid are not observed in time-resolved studies of Pc tautomerization.

Even though the results obtained by steady state fluorescence and transient absorption anisotropy measurements agreed in terms of the important role of tunnelling and the apparent activation energy of the tautomerization reaction, the measured tautomerization rates differed sig-

nificantly. Within the temperature range accessible for both techniques, tautomerization rates in the electronic excited state determined by pump-probe measurements were 200-300 times higher than those obtained with steady-state fluorescence measurements. This discrepancy has not been explained until now. An indication of the reason for so different results obtained by both techniques was brought by single-molecule studies, in which three populations of molecules embedded in a PMMA matrix were identified[48,49]:

- molecules that undergo tautomerization,
- molecules in which tautomerization is blocked and internal hydrogen atoms occupy fixed positions („frozen molecules"),
- molecules which change their state from „frozen" to „hydrogen transferring" on a time-scale of seconds.

Thus, single molecule studies proved that in condensed phase there might be different populations of porphycene molecules that exhibit different behaviours in terms of their ability to undergo tautomerization, whereas in earlier bulk studies it was assumed that the sample is homogeneous. Moreover, single molecule experiments indicated that under certain conditions the medium can govern the double hydrogen transfer process, even though the internal hydrogen atoms seem to weakly interact with their environment[42]. In the present work we shed more light on presence of various populations of porphycene molecules in bulk condensed phases and study effects of their interactions with environment. For this reason we analyze not only anisotropy decay times as in the previous works but also asymptotic anisotropy values. A change of the latter with temperature may result from presence of populations of molecules in the system that are differently affected by their environment[53]. A particular attention was paid to rigid environments such as polymer matrices that can disturb symmetry of guest molecules and affect quantum tunnelling that relies on equivalency of both tautomers[48,49,59]. In order to overcome limitations of earlier experiments and bring applicability windows of fluorescence and transient absorption techniques closer to each other we used a setup based on time-correlated single photon counting which allowed measurements of tautomerization rates in porphycene in the temperature range of approx. 20-170 K with the temporal resolution of approx. 50 ps.

Results and discussion

Steady-state spectroscopy

In the current work we used polymer matrices as media to study the double hydrogen transfer in porphycene. The choice of polymers was dictated by the intention to emphasize the influence of the environment on porphycene tautomerization. On the other hand, we wanted to correlate the results with those of earlier measurements. Thus, the first selected polymer was poly(methyl methacrylate) (PMMA). It allowed preparation of a relatively thick sample (2 mm) of good optical quality, suitable for transient absorption measurements. In PMMA it was, therefore, possible to directly compare the results of earlier transient absorption measurements in non-polar (paraffin oil) and polar (EtOH:MeOH mixture at 4:1 vol. ratio) liquids with the results obtained in a relatively non-polar rigid medium such as PMMA.

The other two polymers used were poly(vinyl alcohol) (PVA) and poly(vinyl butyral) (PVB). These two media were used only in fluorescence studies due to difficulties in obtaining thick non-scattering samples usable in transient absorption measurements.

Room temperature absorption spectra of porphycene in all polymers are typical for that molecule in condensed phases (Fig. 2a). In the region

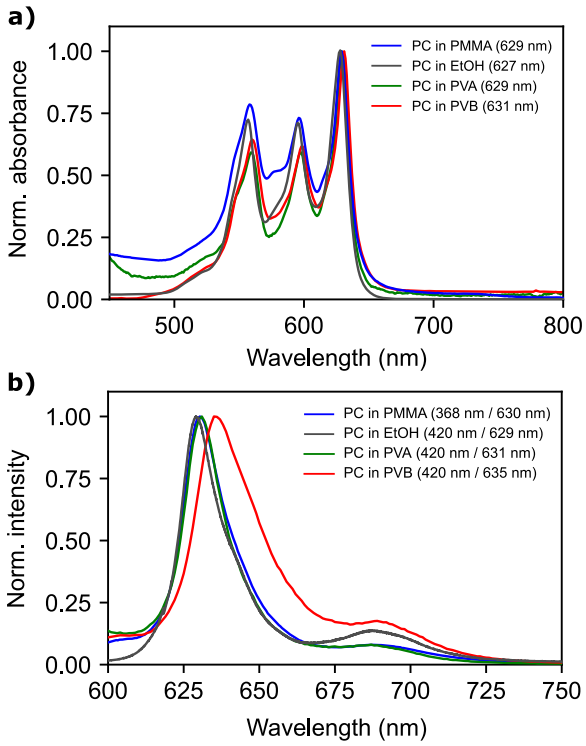

Fig. 2 a) Normalized absorption spectra of porphycene registered in various media (positions of the maxima of the most intense peak are given in parentheses); b) Normalized fluorescence spectra of porphycene registered in various media (excitation wavelengths / positions of the intensity maxima are given in parentheses). The polymers used do not show any fluorescence in the presented wavelengths range.

of the Q-bands they consist of three subbands that are located at approximately the same positions in all media considered here. The red-most subband corresponds to the 0-0 excitation to the first singlet excited state S_1. Wavelengths corresponding to the maximum of this subband (approx. 630 nm) were used to pump and probe samples in transient absorption measurements and to excite them in time-resolved fluorescence studies. The subband located at approx. 565 nm corresponds to the vibronic components of the $S_0 \rightarrow S_2$ transition. Pulses with the central wavelength close to its maximum were used to probe samples in transient absorption measurements in order to avoid probing of the S_1 state through $S_1 \rightarrow S_0$ stimulated emission and to monitor the double hydrogen transfer solely in the electronic ground state S_0.

The central subband, located at approx. 600 nm results from the vibrational progression of the $S_0 \rightarrow S_1$ electronic transition mixed with the origin of $S_0 \rightarrow S_2$ transition. Between the central subband and the 565 nm subband a small additional peak can be noticed in the spectra recorded in PMMA. This peak becomes more noticeable when temperature of the sample is lowered and the bands become narrower (Fig. S1a in the ESI†). At lower temperatures a similar peak located at 575 nm appears also in spectra recorded in PVB (Fig. S1b in the ESI†). This peak indicates presence of aggregated porphycene molecules in PMMA and PVB, however the low degree of aggregation does not prevent tautomerization rate measurements in porphycene monomers.

Flurorescence spectra of porphycene in the studied media are shown in Fig. 2 b. The maxima of all spectra are within 5 nm from each other, with the spectra in PMMA, PVB, and ethyl alcohol almost identical. There are no features that could be clearly attributed to emission of aggregates.

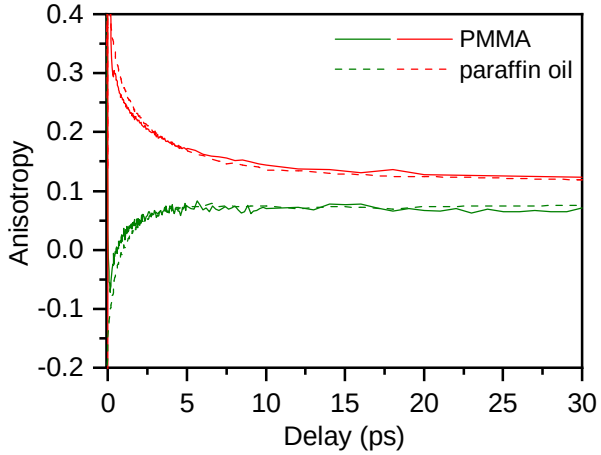

Fig. 3 Room temperature transient absorption anisotropy kinetics recorded for Pc in a PMMA matrix (solid lines) and paraffin oil solution (dashed lines) excited at 630 nm and probed at 630 nm (red) and 550 nm (green). The initial anisotropy in the latter case is equal to approx. -0.2 because at 550 nm the $S_0 \rightarrow S_2$ transition is probed and its dipole transition moment is nearly orthogonal to that of the $S_0 \rightarrow S_1$ transition, as shown in Fig. 1.

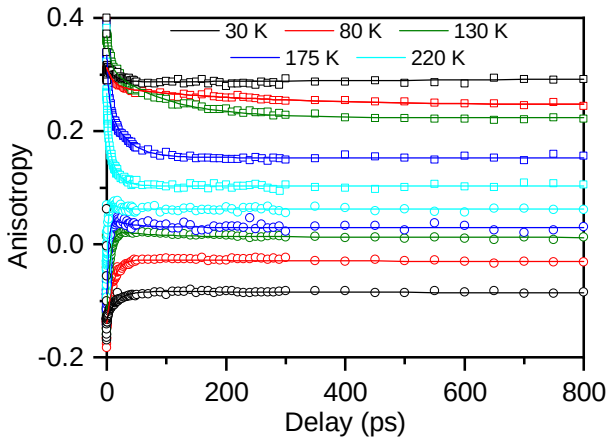

Fig. 4 Kinetics of transient absorption anisotropy recorded for Pc in PMMA at selected temperatures, recorded with probing at 630 nm (squares) and at 550 nm (circles). Solid lines show bi-exponential functions fitted to the data.

Due to very small Stokes shifts the 630 nm probe pulses used in transient absorption measurements coincide with both the absorption and emission maxima. Therefore at this probe wavelength the double hydrogen transfer in both ground and excited electronic states can be monitored because probe pulses tuned to 630 nm interact with S_0 and S_1 states, through absorption and stimulated emission, respectively.

Transient absorption anisotropy measurements

Selected kinetic curves of transient absorption anisotropy recorded at room temperature for Pc in a rigid environment – PMMA matrix – are shown in Fig. 3. They are very similar to those recorded in a liquid environment – paraffin oil. Comparison with another liquid environment used in our earlier studies, EtOH:MeOH mixture at 4:1 vol. ratio, is not straightforward due to a significant contribution of rotational diffusion to the anisotropy kinetics recorded in the latter medium at room temperature. Nevertheless, tautomerization rates obtained by fitting the data with bi-exponential decay functions in all three environments are in good agreement with each other (Table 1). Rate constants measured in both non-polar media, liquid (paraffin oil) and solid (PMMA) are nearly identical, which means that at room temperature the state of matter does not affect the double hydrogen transfer in porphycenes.

Table 1 Anisotropy decay times τ_i and tautomerization rates $k_i = 1/(2\tau_i)$ measured for Pc in different media. Subscripts 0 and 1 refer to the ground state S_0 and the first singlet excited state S_1, respectively

Medium	τ_0 (ps)	τ_1 (ps)	k_0 (10^{11} s^{-1})	k_1 (10^{11} s^{-1})
PMMA	0.90 ± 0.03	6.6 ± 0.4	5.6 ± 0.2	0.76 ± 0.04
Paraffin oil	0.93 ± 0.01	6.3 ± 0.2	5.35 ± 0.06	0.80 ± 0.03
EtOH/MeOH[a]	0.84 ± 0.04	4.9 ± 0.5	5.95 ± 0.30	1.02 ± 0.10

[a] Values obtained by interpolation of data presented in Ref. [46] at temperature 293 K.

Anisotropy decays recorded in PMMA become slower when the sample is cooled down (Fig. 4), as previously observed for Pc in the alcohol mixture [46]. Tautomerization rates obtained by analysing the data according to equations (2) and (4) (effects of rotational diffusion were not observed in PMMA within the temporal window of transient absorption measurements) are shown in Table 2 and presented in the form of an Arrhenius plot in Fig. 5. They are similar to tautomerization rates measured in

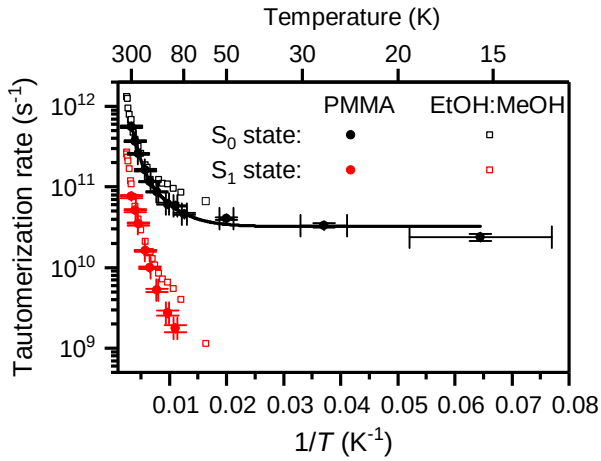

Fig. 5 Arrhenius plots of tautomerization rates of Pc in PMMA obtained by transient absorption anisotropy measurements (filled circles) compared to earlier results obtained in 4:1 vol. EtOH:MeOH mixture (empty squares) [46]. The solid line represents function (5) fitted to the ground state data with E_1 fixed at 0.52 kcal/mol.

the EtOH:MeOH mixture for temperatures above 150 K, however when temperature is lowered below this value they start to differ. The difference could be of methodological origin, because at lower temperatures rotational diffusion time in the alcohol mixture approaches the double hydrogen transfer time, which may lead to incorrect values of the latter obtained by fitting a multiexponential function to the data. On the other hand, the divergence can reflect different properties of both environments that affect the tautomerization process.

The maximum pump-probe delay achievable in the experimental setup for transient absorption anisotropy measurements (up to 1.5 ns) becomes comparable to hydrogen transfer times in the excited state at temperatures below 100 K. Therefore, tautomerization rates in the excited state could be reliably determined by transient absorption anisotropy measurements only at temperatures above approx. 90 K. For this reason the Arrhenius plot for tautomerization of Pc in PMMA in the excited state shown in Fig. 5 could not be analysed (further in this work we discuss tautomerization in the excited state on the basis of time-resolved fluorescence anisotropy measurements). On the other hand, temperature dependence

Table 2 Anisotropy decay times τ_i and tautomerization rates $k_i = 1/(2\tau_i)$ measured by transient absorption anisotropy technique for Pc in PMMA at various temperatures. Subscripts 0 and 1 refer to the ground state S_0 and the first singlet excited state S_1, respectively

Temp. (K)	τ_0 (ps)	τ_1 (ps)	$k_0(10^{10}$ s$^{-1})$	$k_1(10^{10}$ s$^{-1})$
16 ± 3	21 ± 2		2.4 ± 0.2	
27 ± 3	15 ± 1		3.3 ± 0.2	
50 ± 3	12.3 ± 0.4		4.07 ± 0.13	
80 ± 3	10.8 ± 0.3		4.63 ± 0.13	
90 ± 3	8.6 ± 0.2	286 ± 27	5.81 ± 0.14	0.17 ± 0.02
104 ± 3	8.1 ± 0.2	183 ± 14	6.2 ± 0.2	0.27 ± 0.02
128 ± 3	5.75 ± 0.14	96 ± 5	8.7 ± 0.2	0.52 ± 0.03
150 ± 2	4.3 ± 0.1	50 ± 2	11.6 ± 0.3	1.00 ± 0.04
174 ± 2	3.1 ± 0.1	31 ± 1	16.1 ± 0.5	1.61 ± 0.05
221 ± 1	1.94 ± 0.06	14.4 ± 0.7	25.8 ± 0.8	3.5 ± 0.2
246 ± 1	1.35 ± 0.04	9.8 ± 0.4	37.0 ± 1.1	5.1 ± 0.2
295 ± 1	0.90 ± 0.03	6.6 ± 0.4	55.6 ± 1.9	7.6 ± 0.4

of the ground state tautomerization rate, which is measured in PMMA with a relatively high accuracy in the whole studied temperature range, can be very well fitted with a sum of three components:

$$k(T) = a_0 + a_1 \exp\frac{-E_1}{RT} + a_2 \exp\frac{-E_2}{RT} \quad (5)$$

where $k(T)$ is the tautomerization rate measured at temperature T and R is the gas constant. This formula takes into account contributions of three processes to the overall reaction rate:

- tunnelling in the vibrational ground state (rate a_0),
- tunnelling in the first vibrationally excited state of the 180 cm^{-1} mode (preexponential factor a_1, activation energy $E_1 \approx 0.52$ kcal/mol which corresponds to 180 cm^{-1}),
- a process with a higher activation energy E_2 (preexponential factor a_2); Litman *et al.* suggested that this reaction channel corresponds to the stepwise transfer, *via* the short-lived *cis* form, because its activation energy corresponds to the calculated *trans* − *cis* energy difference and the stepwise transfer should be the dominating mechanism at higher temperatures[25].

Two models were used to analyse the data: in the first one all parameters in equation (5) were free, whereas in the other model the lower activation energy was fixed at 0.52 kcal/mol, the value determined in the earlier works[46,54]. The parameters that correspond to the best fit of both models are shown in Table 3. In practice the noise in the data makes the two models indistinguishable and confirms the earlier conclusions on the promoting role of the 180 cm^{-1} vibrational mode in the hydrogen tunnelling in Pc. Tunnelling rates in the vibrational ground state (denoted by a_0 in equation (5)) and in the first excited level of the 180 cm^{-1} vibration (a_1) measured in PMMA are clearly lower then those recorded in the alcohol mixture which may reflect the difference in the Pc-environment interactions. On the other hand the a_1/a_0 ratio is similar in both media therefore the tunnelling enhancement mechanism by the 180 cm^{-1} vibration seems not to be significantly affected by the change of the medium.

Decrease of Pc tautomerization rates with decreasing temperature is accompanied by a significant change of asymptotic values of anisotropy decays. The ratio of the decaying component of anisotropy to its asymptotic value becomes smaller with decreasing temperature. This effect has been also observed during experiments carried out in liquids[46,53], however it is even more pronounced in the data presented here, mainly due to lower temperatures reached in the current study. This effect can be explained if we assume that there exist two populations of molecules in the sample: molecules that undergo tautomerization and molecules that are „frozen", in which the hydrogen transfer is blocked. Such two populations have been observed in single molecule studies of the double hydrogen transfer in Pc and its derivatives in a thin PMMA layer, where molecules undergoing tautomerization and „frozen" molecules could be directly identified[48,49]. Hydrogen transfer freezing can be most probably attributed to distortions of the double potential well by the polymer matrix. The two minima of a distorted well are no longer equivalent, therefore hydrogen atoms become localized in one of them. At room temperature molecules can change their state from „frozen" to hydrogen-transferring, which reflects structural relaxation of the matrix that dynamically changes its influence on guest molecules[48,49].

Presence of two populations is reflected in anisotropy kinetics because the observed anisotropy in such a case is a weighted average of the exponential decay for molecules undergoing tautomerization and the constant value for „frozen" molecules. If we take into account only one electronic state, ground or excited, and denote the fraction of hydrogen-transferring molecules by f, the temporal dependence of anisotropy $r(t)$ will be described by the formula:

$$r(t) = f\left[\frac{r_0 - r_{HT}}{2}\mathrm{e}^{-2kt} + \frac{r_0 + r_{HT}}{2}\right] + (1-f)r_0 \quad (6)$$

where for the electronic ground state $r_0 = 0.4$, and $r_{HT} \approx -0.16$ is the anisotropy value for molecules with hydrogen atoms transferred. The asymptotic anisotropy value equal to

$$r_\infty = f\left[\frac{r_0 + r_{HT}}{2}\right] + (1-f)r_0 \quad (7)$$

increases with the decreasing value of f. Thus, the change of transient absorption anisotropy kinetics observed when the Pc in PMMA sample is cooled can be interpreted as an increase of the number of „frozen" molecules. Knowledge of the temperature dependence of the number of hydrogen-transferring molecules could shed light on the mechanism of the Pc - matrix interactions. In principle equation (7) allows determination of f from anisotropy kinetics, however in transient absorption measurements there are other effects that change anisotropy values. In particular, both ground and excited electronic states contribute to the measured anisotropy kinetics and their wavelength-dependent contributions are difficult to assess in measurements with broadband femtosecond pulses. For this reason we decided to carry out complementary experiments using time-resolved fluorescence measurements. They allow measurements of anisotropy decays in the excited state free from the contribution of the ground state. Moreover, they allow determination of tautomerization rates in the excited state at temperatures below 100 K, where transient absorption measurements fail due to the limited range of pump-probe delays.

Time-resolved fluorescence anisotropy measurements

Fluorescence anisotropy decays recorded for the Pc in PMMA sample (the same as the one used in transient absorption measurements) at selected temperatures are shown in Fig. 6 and Fig. S2 in the ESI† (measurements at temperatures higher than 170 K could not be carried out due to insufficient temporal resolution of the apparatus). Their behaviour resembles that of transient absorption anisotropy kinetics, namely the decays become slower and their asymptotic values become higher when temperature decreases. The fluorescence lifetime of Pc, approximately 11 ns, allows analysis of anisotropy decays up to at least 30 ns. It is apparent that what can be seen as a constant offset in transient absorption anisotropy kinetics is in fact a very slow decay. For this reason fluorescence anisotropy kinetics were fitted not with equation (6) but with its modified version which takes into account two components of the anisotropy decay:

Table 3 Activation energies and preexponential factors obtained by fitting equation (5) to the temperature dependence of tautomerization rates in the electronic ground state S_0 and excited state S_1 determined by transient absorption (TA) and fluorescence anisotropy measurements

Ground state S_0						
Sample	Method	a_0 (10^{10}s^{-1})	E_1	a_1 (10^{11}s^{-1})	E_2	a_2 (10^{12} s^{-1})
PMMA (E_1 free)	TA	3.0 ± 0.6	0.40 ± 0.2 kcal/mol 140 ± 70 cm^{-1}	2.4 ± 2.0	1.8 ± 0.3 kcal/mol 620 ± 100 cm^{-1}	8.4 ± 2.8
PMMA (E_1 fixed)	TA	3.2 ± 0.5	0.52 kcal/mol[a] 182 cm^{-1} [a]	3.9 ± 0.7	1.9 ± 0.2 kcal/mol 670 ± 70 cm^{-1}	9.7 ± 2.8
EtOH:MeOH[46] (E_1 fixed)	TA	6.0 ± 0.2	0.52 kcal/mol[a] 182 cm^{-1} [a]	5.4 ± 0.2	2.5 ± 0.2 kcal/mol 874 ± 70 cm^{-1}	2.3 ± 0.5
Excited state S_1						
Sample	Method	a_0 (10^{8}s^{-1})	E_1	a_1 (10^{10}s^{-1})	E_2	a_2 (10^{12} s^{-1})
PMMA (uncorrected data)	TA+Fluor.	0.89 ± 0.34	0.52 ± 0.14 kcal/mol 183 ± 50 cm^{-1}	1.7 ± 1.7	1.6 ± 0.2 kcal/mol 560 ± 80 cm^{-1}	1.1 ± 0.5
PMMA (temp. corrected[b])	TA+Fluor.	0.84 ± 0.10	0.46 ± 0.04 kcal/mol 163 ± 12 cm^{-1}	1.0 ± 0.3	1.74 ± 0.06 kcal/mol 610 ± 20 cm^{-1}	1.2 ± 0.2
EtOH:MeOH[46] (E_1 fixed)	TA	3.0 ± 1.6	0.52 kcal/mol[a] 182 cm^{-1}[a]	7.7 ± 0.4	2.7 ± 0.2 kcal/mol 944 ± 70 cm^{-1}	7.5 ± 1.4
EtOH:MeOH + PVA (E_1 fixed)	TA+Fluor	28.5 ± 1.7	0.52 kcal/mol[a] 182 cm^{-1}[a]	4.2 ± 0.4	2.2 ± 0.1 kcal/mol 777 ± 30 cm^{-1}	3.9 ± 0.5

[a] value fixed for the fit; [b] temperature scale for TA data shifted by 20 K to compensate for systematic differences in temperature measurements during TA and fluorescence anisotropy measurements

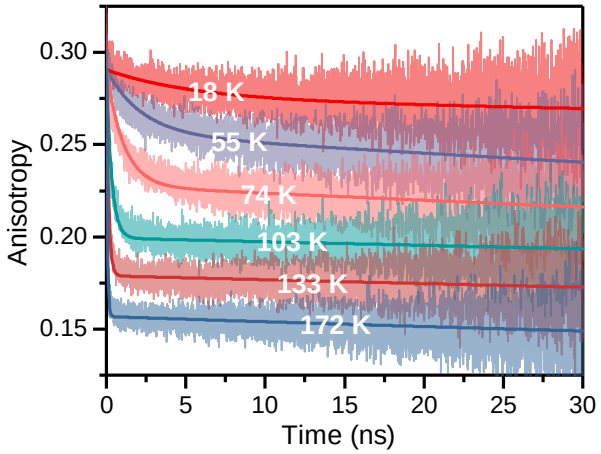

Fig. 6 Fluorescence anisotropy kinetics recorded for Pc in a PMMA matrix at selected temperatures.

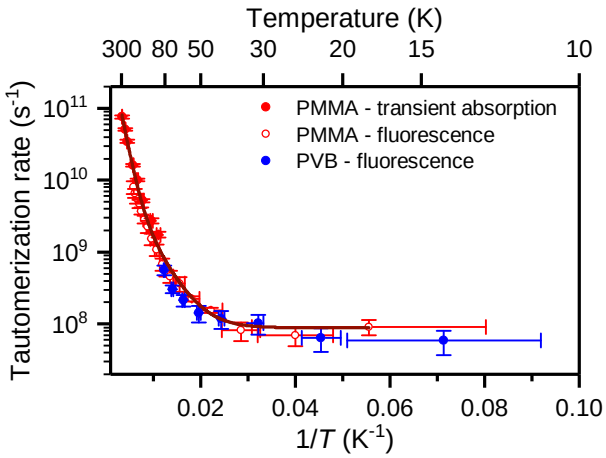

Fig. 7 Temperature dependence of the S_1 state tautomerization rates of Pc in PMMA and PVB measured by transient absorption and fluorescence anisotropy techniques. The solid line represents an Arrhenius-like dependence, given by equation (5) simultaneously fitted to both datasets measured in PMMA.

$$r_t(t) = f r_1(t) + (1-f) r_2(t) \tag{8}$$

$$r_i(t) = \left[\frac{r_0 - r_{HT}}{2} e^{-\frac{t}{\tau_i}} + \frac{r_0 + r_{HT}}{2}\right] = \left[\frac{r_0 - r_{HT}}{2} e^{-2k_i t} + \frac{r_0 + r_{HT}}{2}\right] \tag{9}$$

for $i = 1, 2$. The values of the shorter of the anisotropy decay times (τ_1) obtained by fitting equation (9) to the experimental data and the corresponding tautomerization rates for the „fast" population of Pc molecules in the excited state S_1 are collected in Table 4.

The tautomerization rates are also shown in Fig. 7 together with the rates obtained by transient absorption measurements. The two data sets agree with each other very well, however after a closer look at the graph it appears that they are mutually shifted on the temperature scale. Temperatures for data points obtained by transient absorption measurements seem to be 15-20 K higher than for corresponding data points resulting from fluorescence measurements. Such a systematic offset between real sample temperatures in both experiments is not surprising. First, the pump beam used in transient absorption experiments could locally heat the sample much stronger than the weak excitation beam used in fluorescence measurements. Second, in transient absorption measurements consecutive data points were measured when the sample was cooled, whereas in fluorescence measurements the sample was initially cooled down to the lowest temperature (below 20 K) and measurements were carried out when it was heated. Real sample temperature followed the temperature of the sample holder with a certain delay, thus it could have been higher and lower than indicated by sensors in transient absorption and fluorescence measurements, respectively. In order to take this effect into account the two data sets shown in Fig. 7 were fitted with equation (5) twice: first, without any corrections; second, with the transient absorption data shifted on the temperature scale by 20 K. The curves resulting from both fits are indistinguishable in the scale of Fig. 7 and the obtained parameters are very similar (Table 3). The error limits for parameters obtained in the second case are, however, significantly narrower. Such results make the hypothesis of the systematic temperature shift present in the data very probable. At the same time, they confirm that the obtained values of parameters should be trusted. In both cases the activation energy E_1 corresponding to the tunnelling-promoting vibration (180 cm^{-1}) is well reproduced.

From Fig. 7 it is also clear that the tunnelling rate a_0 in the vibra-

Table 4 Fluorescence anisotropy decay times τ_1 and excited state tautomerization rates $k_1 = 1/(2\tau_1)$ measured by the fluorescence anisotropy technique for Pc in PMMA at various temperatures

Temp. (K)	τ_1 (ps)	k_1 (10^8 s^{-1})
18 ± 8	4400 ± 1300	1.14 ± 0.34
25 ± 5	5700 ± 2200	0.87 ± 0.33
35 ± 5	5400 ± 1800	0.93 ± 0.30
45 ± 5	2920 ± 250	1.71 ± 0.15
55 ± 5	2020 ± 170	2.47 ± 0.20
64 ± 4	1300 ± 310	3.84 ± 0.91
74 ± 4	1030 ± 210	4.85 ± 0.97
84 ± 4	710 ± 140	7.0 ± 1.4
93 ± 4	460 ± 84	10.9 ± 2.0
103 ± 3	331 ± 60	15.1 ± 2.7
113 ± 3	228 ± 42	21.9 ± 4.0
123 ± 3	181 ± 23	27.6 ± 3.5
133 ± 3	146 ± 15	34.2 ± 3.5
142 ± 3	113 ± 14	44.4 ± 5.5
152 ± 2	98 ± 13	51.2 ± 6.8
162 ± 2	83 ± 11	60.3 ± 8.0
172 ± 2	70 ± 13	71 ± 13

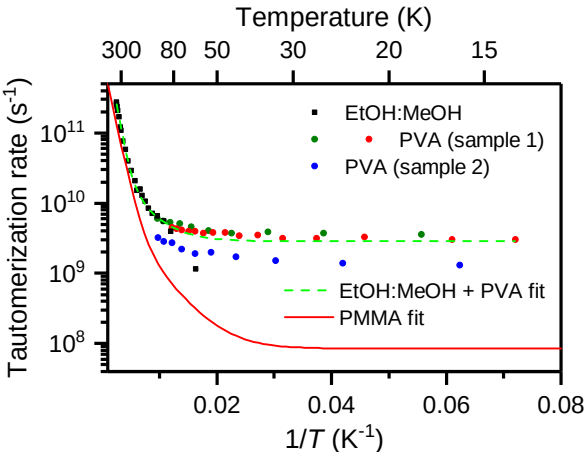

Fig. 8 Temperature dependence of the S_1 state tautomerization rates for Pc in PVA and in the alcohols mixture. Results for two different PVA samples are shown, two fragments cut out of the first sample were independently measured. The green dashed line represents a fit of function given by equation (5) to the merged data sets for the sample 1 in PVA and in the alcohols mixture. The red solid line shows the fit of the data measured in PMMA, as shown in Fig. 7. Error bars are omitted for clarity, the same graph with error bars is shown in Fig. S6 in the ESI†.

tional ground state could not be reliably determined by transient absorption measurements because it is lower than 10^8 s^{-1} – a value far below the applicability range of this technique with the maximum pump-probe delay of 1.5 ns.

The longer of the anisotropy decay times (τ_2) is found to be in the range of 100 ns - 1 μs, therefore it cannot be determined with any reasonable accuracy from the collected data. It has to be mentioned that there are other processes than the double hydrogen transfer that could be potentially responsible for this anisotropy decay. One of them could be rotational diffusion, slowed down, but not completely blocked in the polymer. Nevertheless, reference fluorescence anisotropy measurements of organic dyes in polymer matrices indicated that anisotropy decays, if present, occur on a microsecond timescale at room temperature. Therefore we do not expect an anisotropy decay due to rotational diffusion on a time scale shorter than 1 μs at temperatures below 200 K. The second potential reason for the slow anisotropy decay could be the Förster resonance energy transfer between Pc molecules (homo-FRET). However, the mean distance between Pc molecules in the sample used for the experiments is estimated to be 60 nm and at this distance the efficiency of FRET is negligible. Similarly, the radiative energy transfer due to reabsorption is not expected to play a significant role in the 2 mm thick sample with the absorbance at the maximum of the 635 nm band equal to 0.1 (absorption coefficient at this wavelength $\varepsilon \approx 42000$ M^{-1} cm^{-1})[60]. Nevertheless, we cannot attribute the slow decay to the tautomerization of the „frozen" molecules without any doubts. One of the processes that cannot be excluded is FRET between Pc aggregates that are present in the sample. Therefore we do not draw any conclusions on the tautomerization of „frozen" molecules. Fortunately, the slow component of anisotropy decays is far beyond the time scale of tautomerization of „fast" Pc molecules and on this time scale the slow component can be considered to be a constant offset, as described by equation (6). Therefore, regardless of the nature of this slow component, all conclusions drawn in the previous chapter, in particular the one on the presence of two populations of Pc molecules in rigid media, remain valid.

The results of time-resolved fluorescence anisotropy measurements carried out for Pc in the PVB matrix were very similar to that obtained in the PMMA matrix. As in the previous case, anisotropy decays were bi-exponential with the decay time τ_1 and the excited state tautomerization rate k_1 in a very good agreement with those measured in PMMA (Fig. 7; fluorescence anisotropy kinetics are shown in Fig. S3 in the ESI† and the values of τ_1 and k_1 for Pc in PVB are given in Table S1 in the ESI†). The longer anisotropy decay time was determined to be of the order of 100 ns and thus shorter than that measured in the PMMA sample. This may reflect the fact that concentration of Pc in PVB was higher than in PMMA, which translated to higher absorbance (approx. 0.2) in spite of a thinner sample (approx. 0.3 mm). The mean distance between molecules was estimated as approx. 20 nm. Altogether, this makes radiative and nonradiative energy transfer processes much more efficient in the PVB sample. Thus, they may contribute to the anisotropy decay much more significantly than in the PMMA sample.

The anisotropy decays recorded for Pc in PVA show the same features as those recorded in the samples described above: when the temperature drops, the decays become slower and their asymptotic values increase (Figs. S4 and S5 in the ESI†). There are, however, two significant differences. First, anisotropy decay times and asymptotic anisotropy values change from sample to sample even if the sample preparation procedure is maintained. This effect is not surprising for PVA because this polymer is known to form gels with a porous water-filled structure which strongly depends on parameters such as ambient temperature and the rate of drying of the polymer solution[61–65]. Thus, even changes of temperature and humidity of the surrounding air during sample preparation may affect the microscopic structure of PVA and behaviour of embedded molecules[66,67]. Differences in anisotropy decays observed for different samples prepared according to the same procedure mean that even small changes in the polymer structure, which are beyond our control, can affect Pc tautomerization (because the structure of PVA gels greatly changes as a result of freezing and thawing, care was taken to use each PVA sample only once for cryogenic measurements).

Second, and more importantly, in spite of differences between particular Pc in PVA samples, they all exhibit significantly faster tautomerization rates than the samples prepared in PMMA and PVB for temperatures below 170 K. This difference increases when temperature decreases and the plateau values of the temperature dependence of Pc tautomerization rates are 20-40 times higher in PVA than in PMMA and PVB (Fig. 8). Earlier, we mentioned that tautomerization rates measured by transient absorption anisotropy technique in the alcohol mixture start to differ from those measured in PMMA at approx. 150 K. In comparison with PVA, we can see that the results obtained for the alcohol mixture lie on the same Ar-

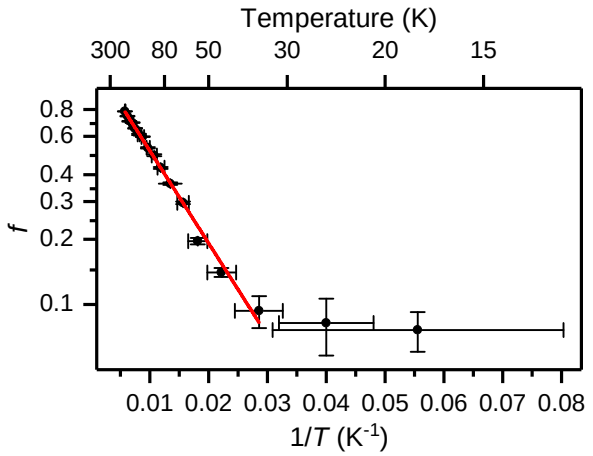

Fig. 9 Temperature dependence of the fraction f of hydrogen-transferring molecules determined for Pc in PMMA. The solid line represents the Boltzmann distribution fitted to the data for temperatures above 35 K ($E = 68 \pm 2$ cm^{-1}).

rhenius curve as the tautomerization rates measured for one of the Pc in PVA samples (parameters of the fitted curve are given in Table 3). Such a good agreement with this particular PVA sample may be a coincidence, however it is apparent that the tautomerization rates in the vibrational ground state of porphycene, given by the a_0 parameter, measured in PVA and obtained by extrapolation of the data for the alcohol mixture alone are much higher than the rates measured in PMMA and PVB. This suggests that the divergence of the transient absorption anisotropy data for Pc in the alcohol mixture and in PMMA is not an artifact resulting from limitations of the technique but a real effect. Therefore, the materials studied here can be divided into two classes:

- PMMA and PVB with the vibrational ground state tautomerization rate in S_1 of approx. $(0.8-0.9)\cdot 10^8$ s^{-1},
- alcohols and PVA with the vibrational ground state tautomerization rate in S_1 in the range of approx. $(1.5-3.0)\cdot 10^9$ s^{-1}.

The difference between a_0 values in these two classes exceeds an order of magnitude. This is an important result, as it shows that the double hydrogen transfer in porphycene is much more sensitive to the properties of the environment than it was thought. Nevertheless, the temperature dependence of tautomerization rates in PVA can be fitted with function 5 with $E_1 \approx 180$ cm^{-1} as in the other media, which means that the mechanism of the vibrationally enhanced tunnelling is always valid, in spite of differences in the properties of the environment.

Because of the range, reliability and reproducibility of the data, further analysis concentrated on the sample prepared in PMMA. Fitting of the function described by equations (8) and (9) to fluorescence anisotropy kinetics allows determination of the fraction of molecules f that undergo „fast" tautomerization, i. e., tautomerization that can be observed by the techniques applied here. Temperature dependence of $f = f(T)$ is shown in Fig. 9 and values of f are collected in Table 5. In the logarithmic vertical and reciprocal horizontal scales the $f(T)$ dependence is nearly linear for temperatures above 35 K. Such a shape of the graph indicates that the $f(T)$ function contains the Boltzmann factor $\exp(-\frac{E}{k_B T})$ and the number of hydrogen-transferring molecules is proportional to the population of an energy state with energy E. The subset of the data for temperatures above 35 K can be very well fitted with a function proportional to the Boltzmann distribution (red curve in Fig. 9):

$$f(T) = f_0 \mathrm{e}^{-\frac{E}{k_B T}} \qquad (10)$$

Table 5 Fraction f of hydrogen-transferring Pc molecules in PMMA determined at various temperatures

Temp. (K)	f
18 ± 8	0.076 ± 0.016
25 ± 5	0.082 ± 0.024
35 ± 5	0.094 ± 0.016
45 ± 5	0.141 ± 0.007
55 ± 5	0.197 ± 0.007
64 ± 4	0.296 ± 0.004
74 ± 4	0.364 ± 0.005
84 ± 4	0.429 ± 0.004
93 ± 4	0.490 ± 0.004
103 ± 3	0.532 ± 0.003
113 ± 3	0.598 ± 0.003
123 ± 3	0.614 ± 0.004
133 ± 3	0.653 ± 0.001
142 ± 3	0.694 ± 0.002
152 ± 2	0.705 ± 0.003
162 ± 2	0.745 ± 0.002
172 ± 2	0.783 ± 0.002

The energy E that corresponds to the best fit is equal to $E = 68 \pm 2$ cm^{-1}. There are no vibrations of such a frequency in porphycene, but this value coincides very well with the peak observed in low frequency Raman spectra of PMMA, located at approx. 70 cm^{-1} [68]. We believe that it is not just an accidental coincidence, but this fact reflects the influence of the environment on the tautomerization process, as mentioned in the Introduction.

The model of tautomerization in rigid environments that emerged from single molecule studies [47–49,59] assumes that the environment disturbs the symmetry of the double potential well and the disturbance is time-dependent due to the polymer reorganization (Fig. 10). The double hydrogen transfer is the fastest when the two minima are isoenergetic because then the tunnelling becomes an efficient reaction channel (validity of this model can be independently confirmed by comparison of tautomerization in symmetric dimers of terephthalic acid [1,3] and asymmetric dimers of ibuprofen [2]). In such a case tautomerization is governed by the dynamics of the environment.

Raman scattering in polymers at low frequencies (below 200 cm^{-1}) arises from the local order (on the scale of a few nanometers) of macroscopically amorphous structures. The commonly accepted model used to describe low frequency Raman scattering in glassy polymers depicts them as structures consisting of highly cohesive regions separated from each other by less cohesive channels [69–72]. This leads to localization of acoustic vibrational modes in separated regions and makes amorphous polymers different in terms of intermolecular vibrations from crystals, in which such vibrations have the form of delocalized and propagating phonons.

When Pc molecules are immobilized in the cohesive regions and their symmetry is disturbed, tunnelling is blocked. Because tunnelling is practically the only tautomerization channel at low temperatures, these molecules are seen as „frozen" in our experiments. Excitation of localized acoustic vibrations allows Pc molecules to regain the symmetry and become hydrogen-transferring. In this model the fraction of hydrogen-transferring molecules should be proportional to the number of vibrationally excited regions. When these regions are separated, they can be treated as independent oscillators and their population can be described by the Boltzmann distribution, as observed in our experiments.

At this point it is worth to recall ground state tautomerization rates calculated by Litman *et al.* [25]. In particular, they calculated the tautomerization rate at 100 K of $6.3 \cdot 10^{10}$ s^{-1}, whereas the value measured by transient absorption in PMMA is equal to $(6.2 \pm 0.2) \cdot 10^{10}$ s^{-1}. Calculations are performed for an undisturbed molecule. Thus, such a good agreement of the calculated and experimental value means that once a molecule is transferred to the hydrogen-transferring population, its tau-

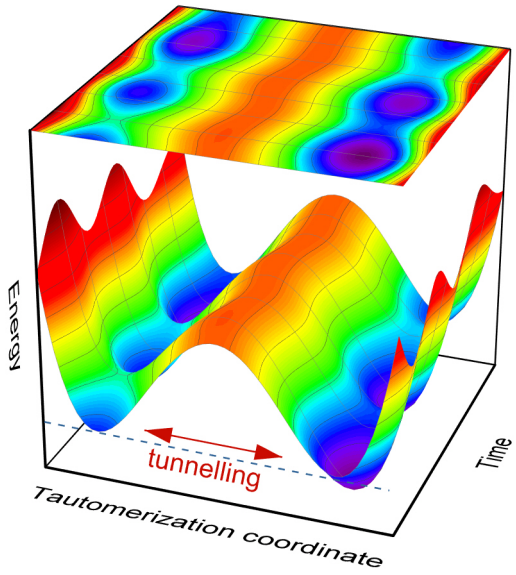

Fig. 10 Model of time-dependent double well distortions that hinder tautomerization through tunnelling until both minima become isoenergetic.

tomerization probability is not significantly affected by the environment. This may be explained by the fact that the classical frequency of polymer intermolecular vibrations is of the order of 10^{12} s^{-1}. 70 cm^{-1} corresponds to approx. $2.1 \cdot 10^{12}$ s^{-1}, a value much higher than the ground or excited states tautomerization rates. Thus, the modulation of the double potential well geometry due to porphycene-polymer interactions occurs on a time scale much shorter than the characteristic time of the hydrogen tunnelling. In such a case it is the rate of the latter that determines the tautomerization rate and the molecule behaves as an undisturbed one.

Extrapolation of the fitted $f(T)$ function indicates that at room temperature over 99% of molecules should undergo tautomerization. This result is in a very good agreement with transient absorption studies, both in PMMA and in solutions, in which asymptotic anisotropy values measured at room temperature correspond to the lack of „frozen" molecules. Thus, it is easy to explain the similarity of tautomerization rates measured in various media at room temperature: nearly all molecules in polymer belong to the „hydrogen transferring" population. Consequently, effects of porphycene-polymer coupling can be seen in bulk samples only at cryogenic temperatures.

In contrast, single molecule studies have shown that at room temperature less than 70% of Pc molecules in PMMA undergo fast tautomerization, significantly less than in bulk studies. When comparing these results we have to take into account the character of the sample used in experiments with single molecules: it was approx. 30 nm thick layer of PMMA spin-coated on a glass slide[49]. The microscopic structure of such a thin layer can be significantly different than that of a bulk PMMA sample. In fact, a large difference between fluorescence lifetimes of hemiporphycene embedded in thin and thick PMMA films has been reported[59]. This result again confirms that tautomerization of porphycene is very sensitive to local microenvironments.

Finally, current results allow explanation of the discrepancy between tautomerization rates obtained from steady-state fluorescence measurements in early works by Gil *et al.*[54] and later time-resolved studies. The estimation of rates from anisotropy of steady-state fluorescence was based on the assumption that all molecules in the sample undergo tautomerization with the same rate and the fluorescence anisotropy results only from the interplay between fluorescence and anisotropy decays. The experiments described above show that this assumption was invalid. Changes of the steady-state fluorescence anisotropy reflect not only changes of the tautomerization rate but also changes of the fraction of hydrogen-transferring molecules f. Nevertheless, it is possible to verify whether the data reported in Ref.[54] also reflect the phenomena that are responsible for the results of time-resolved measurements. In order to do that we calculated „simulated" steady state fluorescence anisotropy using equation (10) from Ref.[54] with the temporal dependence of anisotropy given by equation (6), where experimentally determined values of k (Table 4) and f (Table 5) were substituted. Next, the „tautomerization rates" were calculated from the simulated steady-state anisotropy values using equation (11) from Ref.[54]. The so-obtained values are very similar to the rates reported in Ref.[54] (Fig. S7 in the ESI†), which were based on the directly measured steady-state anisotropy. Thus, the origin of the long-standing discrepancy has been finally identified: it is the presence of two populations of porphycene molecules in the polymer and the temperature dependence of the fraction of molecules that undergo tautomerization. Moreover, it turned out that the steady-state data, seemingly contradictory to the time-resolved data, actually confirm the validity of the model based on the temporal dependence of anisotropy.

Conclusions

We have analysed anisotropy kinetics of transient absorption and fluorescence of porphycene in various polymer matrices at cryogenic temperatures in order to investigate the influence of the environment on the double hydrogen transfer reaction. The results prove that in all studied media the hydrogen tunnelling plays a significant role in the reaction mechanism. Temperature dependence of tautomerization rates indicates that excitation of the 180 cm^{-1} a_g vibration increases the tunnelling rate, as in the previously studied alcohols (EtOH:MeOH) mixture. Comparison of tautomerization rates at temperatures below approx. 150 K shows that at a low temperature the double hydrogen transfer becomes sensitive to properties of the environment. The media used in the low-temperature studies of porphycene tautomerization can be divided into two classes on the basis of the tunnelling rate in the vibrational ground state of the molecule: (1) PMMA and PVB and (2) PVA and EtOH:MeOH mixture. The rate of the vibrational ground state tunnelling in the first class is more than an order of magnitude slower than in the second one.

Analysis of asymptotic anisotropy values proves that there are two populations of porphycene molecules in rigid media, as previously observed in single-molecule experiments: „hydrogen-transferring" molecules, in which tautomerization occurs on time scales below 1 ns and „frozen" molecules in which the double hydrogen transfer cannot be monitored with nanosecond techniques. When temperature decreases more and more molecules become „frozen". This effect can be explained by interactions of guest Pc molecules with a rigid polymer matrix which disturbs the symmetry of the double potential well in porphycene and hinders tunnelling. Temperature dependence of the fraction of hydrogen-transferring molecules suggests that the factor which restores symmetry of porphycene are intermolecular vibrations localized in separated regions of the polymer. It means that porphycene can be an effective probe of the dynamics of its local microenvironment. We also believe that the presented results indicate factors that have to be taken into account in modelling of proton and hydrogen transfer reactions in condensed phase and will provide valuable data for verification of theoretical models.

Conflicts of interest

There are no conflicts to declare.

Experimental section

Synthetic information, details of sample preparation procedures and apparatus used for steady-state and time-resolved spectroscopy measurements are given in the ESI†.

Acknowledgements

This work was supported by the National Science Centre, Poland under Grant No. 2015/16/T/ST2/00355. Piotr Kasprzycki would like to thank D. Birch and P. Yip for the introduction to validated schemes of fluorescence anisotropy measurements. The authors would also like to thank Grażyna Orzanowska for preparation of the samples of porphycene in PVB, Yair Litman for discusions and sharing unpublished results, and Piotr Hanczyc for proof-reading the manuscript.

Notes and references

1 E. A. Pritchina and B. A. Kolesov, Spectrochim. Acta - Part A Mol. Biomol. Spectrosc., 2018, **202**, 319–323.
2 A. G. Demkin and B. A. Kolesov, J. Phys. Chem. A, 2019, **123**, 5537–5541.
3 B. A. Kolesov, J. Phys. Chem. Solids, 2020, **138**, 109288.
4 K. M. Bal, A. Bogaerts and E. C. Neyts, J. Phys. Chem. Lett., 2020, **11**, 401–406.
5 W. J. Bruno and W. Bialek, Biophys. J., 1992, **63**, 689–699.
6 S. Hay, C. R. Pudney, M. J. Sutcliffe and N. S. Scruton, Angew. Chem. Int. Ed., 2008, **47**, 537–540.
7 A. Prah, P. Ogrin, J. Mavri and J. Stare, Phys. Chem. Chem. Phys., 2020, **22**, 6838–6847.
8 P.-O. Löwdin, Rev. Mod. Phys., 1963, **35**, 724–732.
9 O. O. Brovarets' and D. M. Hovorun, J. Biomol. Struct. Dyn., 2015, **33**, 2716–2720.
10 R. Srivastava, Front. Chem., 2019, **7**, 536/1–536/17.
11 J. Li, S. Yang, J. C. Ren, G. Su, S. Li, C. J. Butch, Z. Ding and W. Liu, J. Phys. Chem. Lett., 2019, **10**, 6755–6761.
12 G. Brunton, D. Griller, K. U. Ingold and L. R. Barclay, J. Am. Chem. Soc., 1976, **98**, 6803–6811.
13 D. J. Miller and W. H. Saunders, J. Org. Chem., 1981, **46**, 4247–4252.
14 E. M. Greer, K. Kwon, A. Greer and C. Doubleday, Tetrahedron, 2016, **72**, 7357–7373.
15 P. R. Schreiner, J. Am. Chem. Soc., 2017, **139**, 15276–15283.
16 J. P. Klinman and A. Kohen, Annu. Rev. Biochem., 2013, **82**, 471–496.
17 Y. Xin, A. Huang, Q. Hu, H. Shi, M. Wang, Z. Xiao, X. Zheng, Z. Di and P. K. Chu, Adv. Theory Simulations, 2018, **1**, 1700009.
18 L. Li, B. Fu, X. Yang and D. H. Zhang, Phys. Chem. Chem. Phys., 2020, DOI: 10.1039/d0cp00107d.
19 T. A. Burd, X. Shan and D. C. Clary, Phys. Chem. Chem. Phys., 2020, **22**, 962–965.
20 R. C. Puthenkalathil, M. Etinski and B. Ensing, Phys. Chem. Chem. Phys., 2020, DOI: 10.1039/c9cp06770a.
21 V. Gude, M. Karmakar, A. Dey, P. K. Datta and K. Biradha, Phys. Chem. Chem. Phys., 2020, **22**, 4731–4740.
22 S. Kannath, P. Adamczyk, D. Ferro-Costas, A. Fernández-Ramos, D. T. Major and A. Dybala-Defratyka, J. Chem. Theory Comput., 2020, **16**, 847–859.
23 K. Wang, L. Yang, S. Wang, L. Guo, J. Ma, J. Tang, W. Bo, Z. Wu, B. Zeng and Y. Gong, Phys. Chem. Chem. Phys., 2020, DOI: 10.1039/D0CP01247E.
24 Y. Litman, J. Behler and M. Rossi, Faraday Discuss., 2019, **221**, 526–546.
25 Y. Litman, J. O. Richardson, T. Kumagai and M. Rossi, J. Am. Chem. Soc., 2019, **141**, 2526–2534.
26 H. Liu, J. Cao and W. Bian, Front. Chem., 2019, **7**, 1–10.
27 Z. Smedarchina, W. Siebrand and A. Fernández-Ramos, J. Chem. Phys., 2018, **148**, 102307.
28 Z. Yang, J. Chen, Y. Zhou, H. Huang, D. Xu and C. Zhang, Phys. Chem. Chem. Phys., 2018, **20**, 12157–12165.
29 S. Talukder, P. Chaudhury and S. Ghosh, Int. J. Quantum Chem., 2017, **117**, e25388.
30 Z. Smedarchina, W. Siebrand and A. Fernandez-Ramos, J. Chem. Phys., 2014, **141**, 174312/1–174312/12.
31 D. K. Chakravorty and S. Hammes-Schiffer, J. Am. Chem. Soc., 2010, **132**, 7549–7555.
32 D. K. Chakravorty, A. V. Soudackov and S. Hammes-Schiffer, Biochemistry, 2009, **48**, 10608–10619.
33 S. Hammes-Schiffer, J. Phys. Chem. A, 1998, **102**, 10443–10454.
34 P. M. Kozlowski, M. Z. Zgierski and J. Baker, J. Chem. Phys., 1998, **109**, 5905–5913.
35 Z. Smedarchina, M. F. Shibl, O. Kühn and A. Fernández-Ramoz, Chem. Phys. Lett., 2007, **426**, 314–321.
36 M. K. Abdel-Latif and O. Kühn, Theor. Chem. Acc., 2011, **128**, 307–316.
37 Z. Homayoon, J. M. Bowman and F. A. Evangelista, J. Phys. Chem. Lett., 2014, **5**, 2723–2727.
38 H. H. Limbach, K. B. Schowen and R. L. Schowen, J. Phys. Org. Chem., 2010, **23**, 586–605.
39 J. M. L. D. Amo, U. Langer, V. Torres, M. Pietrzak, G. Buntkowsky, H. M. Vieth, M. F. Shibl, O. Kühn, M. Bróring and H. H. Limbach, J. Phys. Chem. A, 2009, **113**, 2193–2206.
40 U. Langer, C. Hoelger, B. Wehrle, L. Latanowicz, E. Vogel and H.-H. Limbach, J. Phys. Org. Chem., 2000, **13**, 23–34.
41 P. Bernatowicz, Phys. Chem. Chem. Phys., 2013, **15**, 8732–8735.
42 P. Fita, N. Urbańska, C. Radzewicz and J. Waluk, Z. Phys. Chem., 2008, **222**, 1165–1173.
43 P. Fita, N. Urbańska, C. Radzewicz and J. Waluk, Chem. - A Eur. J., 2009, **15**, 4851–4856.
44 P. Fita, P. Garbacz, M. Nejbauer, C. Radzewicz and J. Waluk, Chem. - A Eur. J., 2011, **17**, 3672–3678.
45 P. Ciąćka, P. Fita, A. Listkowski, M. Kijak, S. Nonell, D. Kuzuhara, H. Yamada, C. Radzewicz and J. Waluk, J. Phys. Chem. B, 2015, **119**, 2292–2301.
46 P. Ciąćka, P. Fita, A. Listkowski, C. Radzewicz and J. Waluk, J. Phys. Chem. Lett., 2016, **7**, 283–288.
47 H. Piwoński, A. Hartschuh, N. Urbańska, M. Pietraszkiewicz, J. Sepioł, A. Meixner and J. Waluk, J. Phys. Chem. C, 2009, **113**, 11514–11519.
48 H. Piwoński, A. Sokołowski, M. Kijak, S. Nonell and J. Waluk, J. Phys. Chem. Lett., 2013, **4**, 3967–3971.
49 L. Piatkowski, C. Schanbacher, F. Wackenhut, A. Jamrozik, A. J. Meixner and J. Waluk, J. Phys. Chem. Lett., 2018, **9**, 1211–1215.
50 T. Kumagai, F. Hanke, S. Gawinkowski, J. Sharp, K. Kotsis, J. Waluk, M. Persson and L. Grill, Phys. Rev. Lett., 2013, **111**, 246101–246105.
51 T. Kumagai, F. Hanke, S. Gawinkowski, J. Sharp, K. Kotsis, J. Waluk, M. Persson and L. Grill, Nat. Chem., 2014, **6**, 41–46.
52 J. N. Ladenthin, L. Grill, S. Gawinkowski, S. Liu, J. Waluk and T. Kumagai, ACS Nano, 2015, **9**, 7287–7295.
53 P. Fita, L. Grill, A. Listkowski, H. Piwoński, S. Gawinkowski, M. Pszona, J. Sepioł, E. Mengesha, T. Kumagai and J. Waluk, Phys. Chem. Chem. Phys., 2017, **19**, 4921–4937.

54 M. Gil and J. Waluk, J. Am. Chem. Soc., 2007, **129**, 1335–1341.

55 J. R. Lakowicz, Principles of Fluorescence Spectroscopy, Springer US, Boston, MA, 2006.

56 J. Sepioł, Y. Stepanenko, A. Vdovin, A. Mordziński, E. Vogel and J. Waluk, Chem. Phys. Lett., 1998, **296**, 549–556.

57 E. T. Mengesha, J. Sepioł, P. Borowicz and J. Waluk, J. Chem. Phys., 2013, **138**, 174201.

58 A. Vdovin, J. Waluk, B. Dick and A. Slenczka, ChemPhysChem, 2009, **10**, 761–765.

59 V. Kim, L. Piatkowski, M. Pszona, R. Jäger, J. Ostapko, J. Sepioł, A. J. Meixner and J. Waluk, Phys. Chem. Chem. Phys., 2018, **20**, 26591–26596.

60 J. Waluk, Chem. Rev., 2017, **117**, 2447–2480.

61 F. Yokoyama, I. Masada, K. Shimamura, T. Ikawa and K. Monobe, Colloid Polym. Sci., 1986, **264**, 595–601.

62 S. R. Stauffer and N. A. Peppast, Polymer, 1992, **33**, 3932–3936.

63 H. Trieu and S. Qutubuddin, Polymer, 1995, **36**, 2531–2539.

64 F. Müller-Plathe, J. Chem. Phys., 1998, **108**, 8252–8263.

65 T. Kanaya, H. Takeshita, Y. Nishikoji, M. Ohkura, K. Nishida and K. Kaji, Supramol. Sci., 1998, **5**, 215–221.

66 P. Hanczyc, B. Norden and B. Åkerman, J. Phys. Chem. B, 2011, **115**, 12192–12201.

67 P. Hanczyc, B. Åkerman and B. Nordén, Langmuir, 2012, **28**, 6662–6669.

68 F. Viras and T. A. King, Polymer, 1984, **25**, 899–905.

69 E. Duval, A. Boukenter and T. Achibat, J. Phys. Condens. Matter, 1990, **2**, 10227–10234.

70 F. Viras and T. A. King, J. Non. Cryst. Solids, 1990, **119**, 65–74.

71 A. P. Sokolov, A. Kisliuk, M. Soltwisch and D. Quitmann, Phys. Rev. Lett., 1992, **69**, 1540–1543.

72 A. Mermet, E. Duval, S. Etienne and C. G'Sell, Polymer, 1996, **37**, 615–623.